Reusable, flexible, and lightweight chronic implants for Neuropixels probes

C. BIMBARD[1]*, F. TAKACS[2], J. M. J. FABRE[3], M. D. MELIN[4], N. O'NEILL[3], M. ROBACHA[1], J. S. STREET[3], E. H. VAN BEEST[1], A. K. CHURCHLAND[4], K. D. HARRIS[3], D. M. KULLMANN[3], G. LIGNANI[3], M. CARANDINI[1] & P. COEN[1,5]*

[1]UCL Institute of Ophthalmology, University College London, London, UK
[2]Sainsbury-Wellcome Center, University College London, London, UK
[3]UCL Queen Square Institute of Neurology, University College London, London, UK
[4]Department of Neurobiology, University of California Los Angeles, Los Angeles, California, USA
[5]Department of Cell and Developmental Biology, University College London, London, United Kingdom, UK
*Correspondence: c.bimbard@ucl.ac.uk , p.coen@ucl.ac.uk

Abstract

Understanding neural processes such as memory formation, learning, or aging requires tracking the activity of neural populations across short and long time scales. Such longitudinal recordings can be achieved with chronically implanted Neuropixels probes. An ideal chronic implant should (1) allow stable recordings of neurons for weeks; (2) be light enough for use in small animals like mice; (3) allow reuse of the probes after explantation. In this initial preprint, we present the "Apollo Implant", an open-source and editable device that meets all these criteria and accommodates up to two Neuropixels 1.0 or 2.0 probes. The assembled implant comprises two modules: a recoverable "payload" module, and a "docking" module that is cemented to the skull. The design is readily adjustable: the distance between probes, angle of insertion, and depth of penetration can all be easily changed. We tested the implant across multiple labs, and in head-fixed and freely moving animals. The number of neurons recorded across days was stable, even after repeated implantations of the same probe. The Apollo implant thus provides an inexpensive, lightweight, and flexible solution for reusable chronic Neuropixels recordings.

Introduction

Cognitive processes develop across days (e.g. learning) and behavioral contexts (e.g. social interaction). Therefore, to gain insights into the underlying neural mechanisms, it is necessary to track neural activity across days and contexts. In superficial brain regions, this was made possible with the advent of cellular-resolution imaging techniques (e.g. 2-photon imaging, (Denk et al., 1990; Helmchen and Denk, 2005)). Longitudinal imaging studies have provided significant insights into the evolution of neural processes over learning and context (Driscoll et al., 2017; Lee et al., 2022). However, most imaging techniques fail to capture fast neural dynamics, and accessing deep brain regions can require invasive surgery (Dombeck et al., 2010; Mizrahi et al., 2004). Electrophysiology overcomes these issues, and substantial effort has thus been dedicated to developing chronic implants for electrophysiology recordings (Berényi et al., 2014; Ferguson et al., 2009; Shobe et al., 2015). But these implants typically record a relatively small number of neurons, whereas cognitive processes are increasingly thought to be encoded across large neural populations (Pinto et al., 2019; Steinmetz et al., 2019; Tseng et al., 2022; Urai et al., 2022).

With newly developed Neuropixels probes, many hundreds of neurons can be recorded in a single insertion (Jun et al., 2017; Steinmetz et al., 2021). Using these probes, experimenter have produced brain-wide maps of behaviors in head-restrained mice using acute recordings (Allen et al., 2019; International Brain Laboratory et al., 2023; Steinmetz et al., 2019; Stringer et al., 2019). Acute recordings are not suitable for tracking neural activity of the same cells across days or behaviors. To this end, several solutions for the chronic implantation of these probes have been proposed, including permanent (Jun et al., 2017; Steinmetz et al., 2021) and recoverable (Aery Jones, 2023; Juavinett et al., 2019; Luo et al., 2020; Steinmetz et al., 2021; van Daal et al., 2021) implants. Remarkably, chronic implants were recently used to track neurons across many weeks

(Steinmetz et al., 2021). The permanent implants used in these experiments are lightweight and very stable, but their use on a large scale is not financially feasible. Conversely, recoverable implants can be reused, but further efforts are needed to find solutions that are cheaper, lighter, more flexible, and easier to implant and explant. In particular, the only published recoverable implant for Neuropixels 2.0 probes is too heavy for use with typical mice, especially in its dual-probe form, and cannot be adjusted for different implantation trajectories (Steinmetz et al., 2021; van Daal et al., 2021).

To address these issues, we developed the "Apollo implant" (named for its modular design) for the reversible chronic implantation of Neuropixels probes. It comprises two modules: the recoverable payload module accommodates up to two Neuropixels probes and is reused across animals, and the docking module is permanently cemented to the skull during implantation. The design is open source and can be readily adjusted to change the distance between probes, implantation depth, or angle of insertion.

Five laboratories have already used, or are in the process of testing, the Apollo implant in setups that use both mice and rats. Three of these groups have provided data for this initial preprint. The same Neuropixels probes have been reimplanted up to 6 times with no significant change in recording quality. Recordings were stable across weeks and sometimes months. This allows for recordings to cover the entirety of 2.0 probes, while minimizing set-up time, and could facilitate the tracking of neurons across days. The design has been independently printed, adjusted, and implanted across multiple labs, and implanted subjects included freely behaving mice and rats and head-fixed mice, with both 1.0 and 2.0 probes.

Results

Flexible design

The Apollo implant consists of two complementary parts, the payload and the docking modules, inspired by previous designs (van Daal et al., 2021) (Figure 1). Both parts can be 3D-printed in a variety of materials, although we typically used a combination of Nylon PA12 and Formlabs Rigid Resin. The Neuropixels 1.0 and 2.0 implants weigh ~1.6 g and ~1.4 g. This is ~37% lighter than the only published Neuropixels 2.0 solution (van Daal et al., 2021; Steinmetz et al., 2021). Payload modules can accommodate up to 2 parallel probes , each of which adds a further 0.45 g and 0.19 g for 1.0 and 2.0 versions. The electronics are protected by two lids with protective slots to accommodate the flex-cables when not connected to the headstage (Figure 1A). To ensure the implant is maximally compact, flex cables are folded into the cavity beneath the lids (Figure 1B). This minimizes the height of the implant, reducing the moment of inertia above the animal's head. The entire implant can be 3D-printed for ~$10 (~$3 for each disposable module).

The implant is flexible and recoverable, allowing the same Neuropixels probe(s) to be used multiple times and in different configurations (Figure 1C). Once the payload module is constructed, the distance between the two probes remains fixed. The docking module is connected to the payload module via small screws, which makes it easy to assemble, and disassemble upon explantation. Only the docking module is cemented to the animal's skull, and it is covered with merlons to increase contact with the cement and therefore the stability of the implant. To facilitate different implantation depths and angles with the same payload module, both the length and base-angle of the docking module can be adjusted. The base of the implant thus remains parallel to the skull (Figure 1C) which improves stability and reduces weight by minimizing implant-height and the quantity of cement required. All adjustments can be easily achieved by inexpert CAD users with the preset parameters supplied in the editable files (Supplementary Video 1).

To help combine the payload and docking modules, we designed a dedicated constructor (Figure 1D). The docking holder, containing a new docking module, slides onto the constructor posts, and the payload holder, containing the payload module, is fixed to the end. The two modules are thus coaxial, and the docking module can slide into position and be secured to the payload module without risk of damaging the probes. The constructor comprises 3D-printed parts and Thorlabs 6 mm poles for a one-time cost of ~$25.

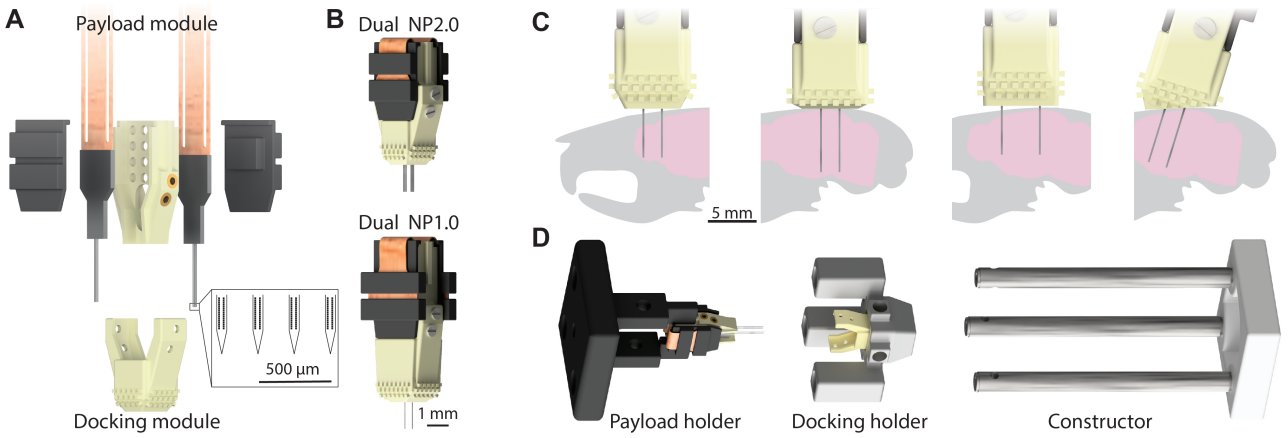

Figure 1. The Apollo implant has a flexible design. A. Exploded view of the implant, showing the two modules: the payload module, which accommodates up to two Neuropixels probes (protected by two lids), and the docking module. Zoom-in: scaled illustration of the tip of a 4-shank Neuropixels 2.0 probe. Each shank is 75 µm wide, with 250 µm center-center distance between shanks and 15/32 µm vertical/horizonal distance between electrode sites on each shank. **B**. Assembled view of the implant, for 2.0 (top) and 1.0 (bottom) probes. **C**. Illustration of implant flexibility. Compared with the standard model (left), the length of exposed probes (middle-left), spacing between probes (middle-right), and implantation angle (right) can all be adjusted with preset parameter changes in the software files (Supplementary Video 1). **D**. Constructor for the assembly of the payload and docking modules. The docking holder slides along the posts of the constructor, and optimally aligns with the payload module being held by the payload holder. This effectively eliminates the risk of breaking the shanks when combining modules.

Stability

We tested the stability of the Appollo implant with both Neuropixels 1.0 and 2.0 probes (Figure 2). We implanted 31 mice using single or dual 4-shank Neuropixels 2.0 implants, and two Neuropixels 1.0 implants (one single and one dual), over a period of days to months. The probes were typically inserted 5-6 mm, traversing multiple brain regions (Figure 2A,B). Because only 384 of the 5120 channels, termed a “bank” of channels, can be recorded simultaneously on each probe, multiple recording sessions were used to cover all channels in the brain. Compared with acute recordings, this strategy dramatically reduces experimental set-up time and complexity, and is especially beneficial for whole brain approaches. The raw signal quality did not significantly change across days (Figure 2C,D), allowing us to identify single spikes reliably for months. The spiking patterns on each probe were similar across days (Figure 2E,F), suggesting that the same populations of neurons were being tracked and that minimal drift occurred.

The number of recorded neurons was stable across weeks. For each session, we quantified the number of well-isolated single units for each individual channel bank (Figure 3A). Units were selected based on stringent criteria, including amplitude, percentage of missing spikes, and refractory period violations. To obtain the total number of single units for each probe, we summed units across all banks within the brain (Figure 3A). The number of single units could remain stable for more than 50 days, and we observed comparable stability in most of mice (Figure 3B). As previously described (Luo et al., 2020), we often observed an initial fast decrease in unit-number, but this was not systematic. Indeed, in some animals, the number of units increased slowly until reaching a peak after 20-30 days (Figure 3A). The mean decrease in unit count per day was ~6% (median 4%), within the range previously observed for permanent and recoverable implants (Steinmetz et al., 2021). Unit decrease did not depend on the number of times a probe was reimplanted (p-value = 0.81, linear mixed effects model, Figure 3C), or on the insertion coordinates of probe (p-value = 0.39, linear mixed effects model, Figure 3D). However, implant quality was more variable in posterior brain regions, with instances of rapidly decreasing neuron counts, as previously described (Luo et al., 2020). In all but one animal—where infection compromised skull integrity and one probe was broken during or before explantation—all probes were explanted successfully, representing ~97% recovery rate.

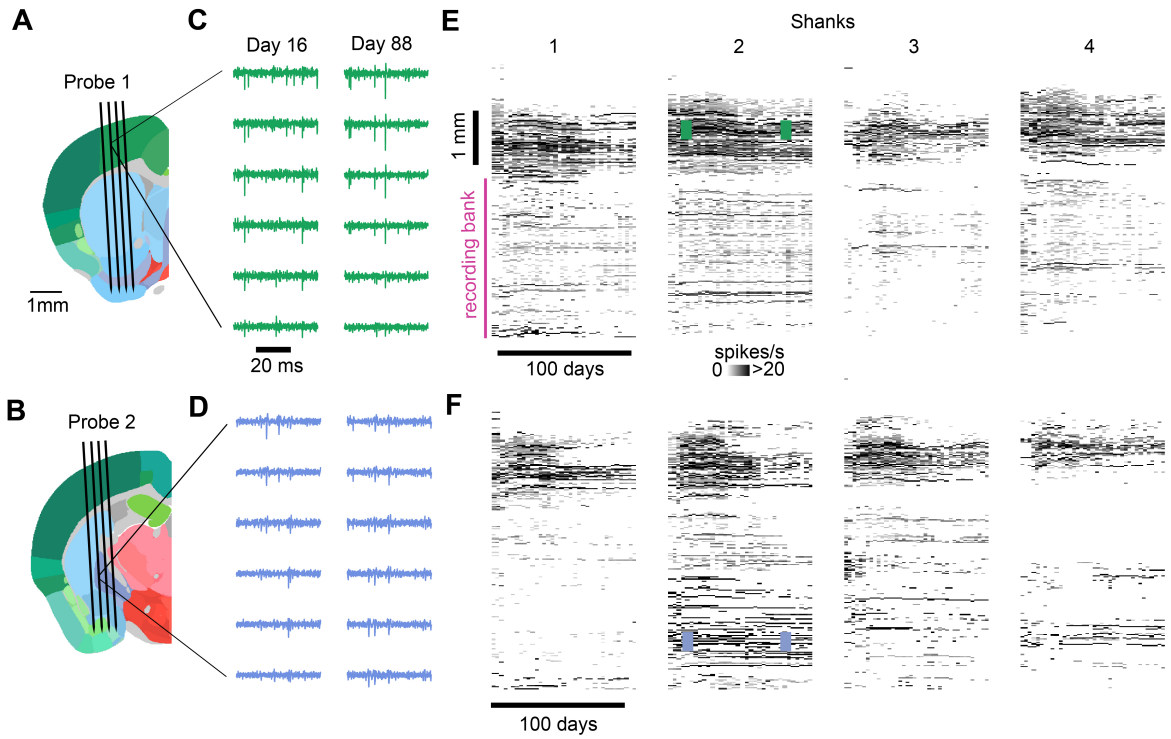

Figure 2. The Apollo implant provides good-quality signal over weeks. **A,B.** Insertion trajectories of two simultaneously implanted 4-shank Neuropixels 2.0 probes, with respect to brain anatomy (Allen Mouse Brain Atlas, (Wang et al., 2020)). **C,D.** Raw signal (bandpass filtered between 400Hz and 9kHz) across 6 channels, on day 16 and 88 post-implantation. **E,F.** Number of spikes per second versus depth along the probe (y-axis) and days from implantation (x-axis) for the same implantation shown in A-D. The total number of spikes per second (across all detected units) is binned across depths for each day (20 µm bins).

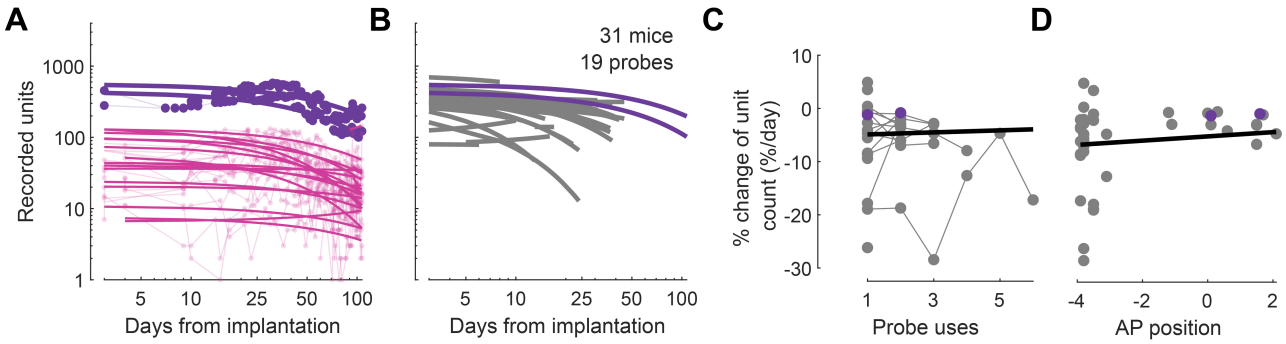

Figure 3. The Apollo implant is stable across days. A. Total number of recorded units across days for individual channel banks (pink), and across each probe (purple), for the same implantation as in Figure 2. Lines: logarithmic fits. **B**. Logarithmic fits across all implantations (purple, implantation from Figure 2). Of the 31 animals, two were implanted with Neuropixels 1.0 probes (one dual and one single implant). **C.** Change in unit count versus number of implantations. Connected dots represent single probes, reused up to 6 times. The slope is quantified with a linear mixed-effects model (thick line). **D**. Decrease in unit count versus antero-posterior position of the insertion, relative to bregma.

Freely behaving animals

To test whether the Apollo implant could be used in more naturalistic conditions, we recorded from a freely behaving mouse with a single Neuropixels 1.0 implant (Figure 4). The mouse freely explored its home cage (Figure 4A), suggesting that the weight and momentum of the implant—which are further reduced for the Neuropixels 2.0 version—did not impair movement. The recording yielded high-quality, well-isolated single units for weeks (Figure 4C). These preliminary results suggest the Apollo implant can be used to record large populations of neurons, with minimal noise, during unrestrained behavior.

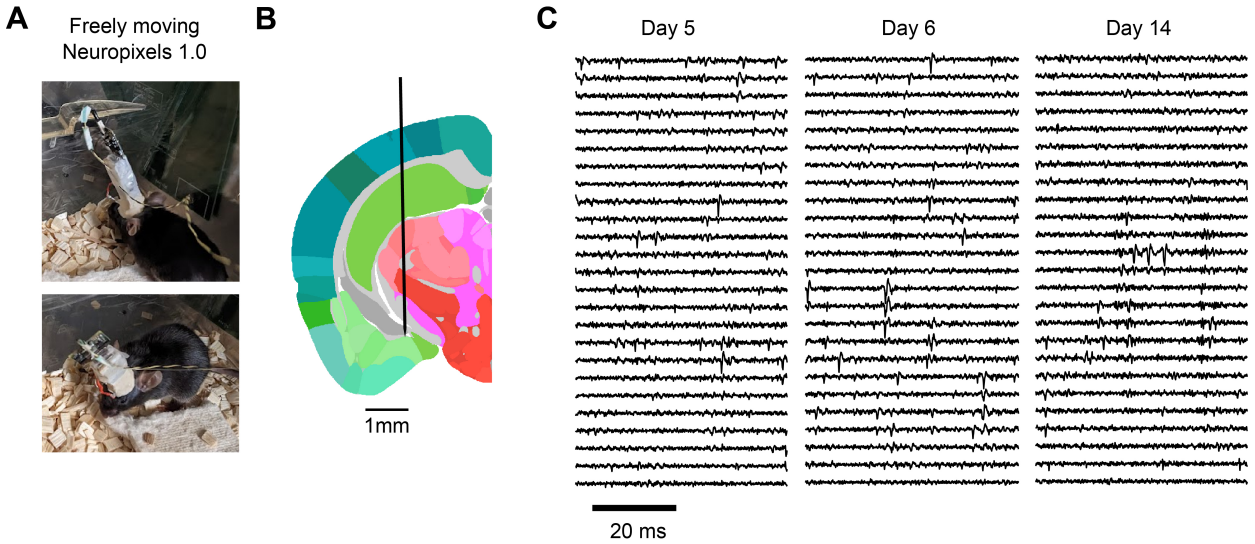

Figure 4. The Apollo implant can be use in freely behaving animals. A. Animal freely-moving with the Apollo implant. **B**. Insertion trajectory of the Neuropixels 1.0 probe. **C**. Raw signal (bandpass filtered between 400Hz and 9kHz) across multiple channels of increasing depth, on days 5, 6 and 14 post-implantation.

Discussion

To record large populations of neurons across days and during natural behaviors we developed the "Apollo implant": a chronic implant for Neuropixels 1.0 and 2.0 probes. Our solution is easily implanted and recovered, inexpensive, lightweight, flexible, and stable. We tested the implant across multiple labs and setups (head-fixed or freely moving), recording neural populations across weeks, and even months.

The design of the Apollo implant builds upon past advances in chronic devices (Juavinett et al., 2019; Luo et al., 2020; Steinmetz et al., 2021; van Daal et al., 2021) to improve on several aspects: weight, price, flexibility, and ease of use. The implant is optimized for small animals, like mice, which cannot carry heavy loads (especially female and water-deprived animals). Because the headstage is not permanently fixed to the implant, the weight carried by the animal outside of recordings is reduced, and multiple animals can be sequentially recorded with a single headstage. The implant is strong enough to be carried by rats (data not shown), but its use in stronger animals, like ferrets or monkeys, remains untested. For applications requiring even lighter implants, such as birds, a different printing material can be used to further reduce the weight by ~40% (see Methods), although we have not tested for the stability of such implants.

The Apollo implant is more flexible than previously published solutions. A unique aspect of our modular design is that different docking modules can be used when reimplanting the same payload module. The provided CAD files are fully editable and open source, allowing experienced users to modify the parts as needed. For inexpert users, the files are populated with predefined key dimensions that can be easily adjusted to accommodate changes in several features, including inter-probe distance, angle of implantation, and the length of exposed probes. This flexibility ensures the implant remains close to the skull for each experiment, minimizing surgical complications, implant weight (less bonding agent is needed), and moment of inertia (height is minimized).

With the Apollo implant, the number of recorded neurons exhibited good stability across days, regardless of the number of times the probe had been reimplanted. To provide a realistic estimate for the number of high-quality units that could be recorded across days, we used stringent quality metrics based on unit waveform and spiking properties. Predicting the stability of an implantation was difficult and did not seem to correlate strongly with the quality of surgery (e.g. a small bleed during craniotomy, or ease of probe insertion). We observed more variable stability at the back of the brain, especially in superior colliculus, possibly due to the mechanical constraints imposed during head movements.

We have not tracked neurons across days in this preliminary preprint. However, this is feasible with chronic Neuropixels implants (Steinmetz et al., 2021), and we are currently testing different methods with this data. Together these methods will be essential to fully understand cognitive processes that evolve over longer timescales, such as learning or aging.

Overall, we believe the Apollo implant fills an important niche to facilitate chronic electrophysiology with Neuropixels probes, particularly in small animals. Increasing the diversity and versatility of chronic implants will allow researchers to choose the solution most suited to their experimental needs.

Acknowledgements

This work was supported by the Biological Sciences Research Council (BB/T016639/1 to MC and PC), Wellcome Trust (110120, 205093 and 204915 to PC, MC and KDH), the European Union's Horizon 2020 research and innovation program (694401 to KDH), the European Molecular Biology Organization (ALTF 740-2019 to CB), The Simons Collaboration on the Global Brain (AKC), the National Institutes of Health (U19NS123716**,** AKC, MM), and the Medical Research Council (MR/V034758/1 to DMK and GL). FT is supported by the Sainsbury Wellcome Centre PhD program and JMJF is supported by a Wellcome Trust PhD Studentship. MC holds the GlaxoSmithKline/Fight for Sight Chair in Visual Neuroscience.

Author contributions

	Bimbard	Takacs	Fabre	Melin	O'Neill	Robacha	Street	van Beest	Churchland	Harris	Kullmann	Lignani	Carandini	Coen
Conceptualization	●												●	●
Methodology	●	●												●
Software	●	●	●											●
Formal Analysis	●													
Investigation	●	●		●	●	●	●	●						
Writing -- Original Draft	●													●
Writing -- Review & Editing	●	●	●	●	●		●	●	●		●	●	●	●
Visualization	●													●
Supervision									●	●	●	●	●	●
Funding Acquisition	●								●	●	●	●	●	●

Methods

Experimental procedures at UCL were conducted according to the UK Animals Scientific Procedures Act (1986) and under personal and project licenses released by the Home Office following appropriate ethics review.

Experimental procedures at UCLA conformed to the guidelines established by the National Institutes of Health and were approved by the Institutional Animal Care and Use Committee of the University of California, Los Angeles David Geffen School of Medicine.

Implant design and materials

All parts of the implant (except the constructor probes, Thorlabs) were designed using Autodesk Inventor Professional 2023 software, acquired free of charge through the renewable education plan. Parts were 3D-printed by external companies (SGD 3D, https://sgd3d.co.uk/). Stereolithography (SLA, using Tough4000 rigid resin, Formlabs) was used for the payload and docking modules, the docking holder, and the constructor head. Selective laser sintering (SLS, using Nylon PA12) was used for the payload module lids and payload holder.

Brass threaded inserts were manually added to the payload module, payload holder, and docking holder using a soldering iron after printing. For parts (e.g. the payload and docking modules) where strength and inflexibility were advantageous, we used Tough4000 rigid resin, although this material is denser than Nylon PA12. With this combination, the Neuropixels 1.0 and 2.0 implants weighed ~1.6 g and ~1.4 g. The weight of the implants could be further reduced to 1.1 g and 1.0 g if the payload and docking modules were also printed with Nylon PA12. While we do not anticipate a reduction in recording quality or stability when constructing the entire implant from Nylon PA12, this remains untested.

Implant assembly and preparation

Carandini-Harris laboratory – payload module assembly

The payload modules were assembled with either one or two 4-shank Neuropixels 2.0 probes. The empty payload module was positioned on Blu Tack and coated with a thin layer of epoxy (Araldite). The probe was then affixed and aligned to the payload module, either by eye or using graph paper, before covering the base and electronics with epoxy. The ground and reference were shorted by connecting them with a silver wire. The flex cable was folded and inserted into the slot on the inside of the lid before the lid was glued to the payload module with superglue (Loctite). The probe was then sharpened using the payload holder and a microgrinder (Narishige EG-45). In the case of dual implants, the second was sharpened using a separate holder and then affixed, through the same procedure, to the other side of the payload module. The ground/reference of the probes were connected.

Churchland laboratory – payload module assembly

The payload modules were assembled with two Neuropixels 1.0 probes. The probes were first sharpened individually (Narishige EG-45). We then checked probe alignment in the holder without any cement or glue. Kapton tape was added to the backside of the probes and then alignment was rechecked to ensure a straight shank trajectory. After verifying proper alignment, the probes were affixed to the payload module, before covering the base and electronics with light curable dental cement (SDI, Wave A1). UV light was applied to cure the cement. The ground and reference were shorted by connecting them with a silver wire. This wire was then soldered to a socket connector (Digikey, ED5164-15-ND) to allow for grounding with a bone screw. A bone screw tethered to its own socket connector was also prepared to allow for detachment of the grounding screw from the probes at the conclusion of the experiment. The flex cable was folded and inserted into the slot on the inside of the lid before the lid was glued to the payload module with UV cement (SDI, Wave A1).

Kullman/Lignani laboratories – payload module assembly

Payload modules were assembled with one Neuropixel 1.0 probe. The payload module was positioned on BluTack. A thin layer of epoxy resin (Araldite Rapid Liquid Adhesive, ARA-400007) was applied to the base of the payload module and the probe was affixed. Additional epoxy resin was applied around the edge of the probe base. The probe ground and reference were shorted with 0.5 mm silver wire (Sigma Aldritch 265586-100cm). This short was soldered to an additional silver wire, terminated with a male Mill-Max pin and insulated with Plastidip, for connecting to a skull ground screw during recordings. The probe was then sharpened using the payload holder and a microgrinder (Narishige EG-45). The flex cable and ground wire were folded so as to be contained within the payload module and two 3D-printed lids were glued (RS Pro Super-glue) to each side.

All laboratories – implant assembly

For each implantation, a new or previously used payload module was combined with a new docking module. The docking module was positioned in the docking module holder and secured in place with set screws. This holder was slid onto the arms of the constructor. The payload module (with probes) was secured in a payload module holder and attached to the end of the constructor with screws. Finally, the docking module holder was slid along the constructor arms toward the payload module, and the two modules were secured with screws.

Before each implantation probes were coated with DiI (Vybrant V22888 or V22885, ThermoFisher) by either manually brushing each probe with a droplet of DiI or dipping them directly in DiI.

Implantation

Carandini-Harris laboratory

A brief (approximately 1 h) initial surgery was performed under isoflurane (1–3% in O2) anesthesia to implant a titanium headplate (approximately 25 × 3 × 0.5 mm, 0.2 g). In brief, the dorsal surface of the skull was cleared of skin and periosteum. A thin layer of cyanoacrylate (VetBond, World Precision Instruments) was applied to the skull and allowed to dry. Thin layers of UV-curing optical glue (Norland Optical Adhesives #81, Norland Products) were applied and cured until the exposed skull was covered. The head plate was attached to the skull over the interparietal bone with Super-Bond polymer (Super-Bond C&B, Sun Medical). After recovery, mice were treated with carprofen for three days, then acclimated to handling and head-fixation.

Craniotomies were performed on the day of the implantation, under isoflurane (1–3% in O2) anesthesia, and after injection of Colvasone and Carprofren. In brief, the UV glue was removed, and the skull cleaned and scored for best adhesion of the cement. The skull was levelled, before performing the craniotomies (craniotomy in the case of single-probe implants) using a drill or a biopsy punch. Once exposed, the brain was covered with Dura-Gel (Cambridge Neurotech).

The implant was held using the 3D-printed payload holder and positioned using a micromanipulator (Sensapex). After positioning the 8 shanks at the surface of the brain, avoiding blood vessels, probes were inserted at slow speed (3-5 µm/s). Once the desired depth was reached (optimally just before the docking module touched the skull), the implant was sealed using UV cement (3M RelyX Unicem 2 Automix), then covered with Super-Bond polymer, ensuring that only the docking module was cemented.

Churchland laboratory

Headbar implantation and Neuropixels implantation were performed within the same surgery. In brief, the dorsal surface of the skull was cleared of skin and periosteum. A thin layer of cyanoacrylate (VetBond, World Precision Instruments) was applied to the edges of skull and allowed to dry. The skull was then scored with a scalpel to ensure optimal adhesion. After ensuring the skull was properly aligned within the stereotax, craniotomy locations were marked by making a small etch in the skull with a dental drill. A titanium headbar was then affixed to the back of the skull with a small amount of glue (Zap-a-gap). The headbar and skull were then covered with Metabond, taking care to avoid covering the marked craniotomy locations. After the Metabond was dry, the craniotomies for the probes and grounding screw were drilled. Once exposed, the brain was covered with Dura-Gel (Cambridge Neurotech).

The implant was held using the 3D-printed payload holder and positioned using Neurostar stereotax. After positioning the shanks at the surface of the brain, avoiding blood vessels, probes were inserted at slow speed (5 µm/s). Once the desired depth was reached, an additional layer of Kwik-Sil was applied over the craniotomy and the implant was sealed using UV cement (SDI, Wave A1). It was then covered with Metabond, ensuring that only the docking module was cemented. After recovery, mice were treated with meloxicam and enrofloxacin for three days, then acclimated to handling and head-fixation.

Kullman/Lignani laboratories

The mouse underwent a single surgery for implantation of the Apollo implant. The animal was anaesthetised (isoflurane in O2, 4% induction, 0.5-3% maintenance) and given appropriate analgesia (buprenorphine, 4.5 micrograms SC). The animal was head-fixed in a stereotaxic frame and topical lidocaine/prilocaine (Emla 5%) and beta-iodine were applied to the scalp. The dorsal surface of the skull was exposed and cleared of connective tissue and periosteum. A 0.7 mm burr hole was made on the left (contralateral) parietal skull plate and a skull screw (with 0.5mm silver wire, terminating at a female Mill-Max pin) was inserted. A craniotomy

was made above the implant site (AP -2 mm, ML +1.8 mm from bregma) using a 1.5 mm biopsy punch (Integral) and bur (R&S Diamond Bur Taper Conical End Super Fine, Z12). Any bleeding was stemmed with a haemostatic sponge soaked in saline. Dura-Gel (Cambridge Neurotech) was applied into the craniotomy and allowed to cure for 30 minutes. A thin layer of Medbond glue was applied to the surface of the skull at the sutures to adhere the skull bones together and around the skin perimeter to adhere the surrounding skin to the skull.

The Apollo implant was held on the stereotaxic frame in the payload holder and the shank was positioned in the center of the craniotomy. The shank was lowered through the dura and into the brain at a slow speed (3-5 µm/s) using a micromanipulator (Sensapex uMp-4) to the target depth (DV -5.375 mm). Once positioned, bluelight-curing cement (3M RelyX Unicem 2) was applied to affix the base of the docking module to the skull. The skull, docking module, and ground screw and wire were then covered with dental resin cement (Super-Bond). Once the cement had fully dried, the gold contacts of the probe's ZIF connector were protected with a small strip of parafilm, and another strip of parafilm was wrapped at the top of the implant.

At the end of the surgery, the animal was given meloxicam (Metacam, 30 micrograms SC), 20% glucose in saline (0.2 ml SC), and amoxicillin (Betamox, 15 mg SC). The animal was allowed to awaken on the heating mat before being placed in a heated recovery box and then returned to its home cage.

Explantation

All laboratories

The probes were explanted using the 3D-printed payload holder. With a micromanipulator, the holder was aligned to the payload module, slid into place, and secured with a screw. The screws between the payload and the docking modules were then removed, and the payload module extracted. Once extracted, probes were sometimes contaminated with debris, like Dura-Gel or biological tissue. Extensive cleaning with Tergazyme (24h) and de-ionized water typically cleaned the probes without altering the signal quality. If this procedure proved insufficient, a 24h bath in a stronger detergent (DOWSIL DS-2025 Silicone cleaning solvent) removed the residual tissue.

Carandini-Harris & Churchland laboratories

After explantation, brains were imaged using serial section two-photon tomography (Mayerich et al., 2008; Ragan et al., 2012). The microscope was controlled by ScanImage Basic (Vidrio Technologies) using BakingTray (https://github.com/SainsburyWellcomeCentre/BakingTray, https://doi.org/10.5281/zenodo.3631609). Images were assembled using StitchIt (https://github.com/SainsburyWellcomeCentre/StitchIt, https://zenodo.org/badge/latestdoi/57851444). Probe location was checked visually or using brainreg (Claudi et al., 2020; Niedworok et al., 2016; Tyson et al., 2022).

Kullman/Lignani laboratories

Following explantation, the animal was culled with an overdose of pentobarbitol (Pentoject 200mg/ml) while under anesthesia and the brain was extracted for histological processing and confirmation of probe trajectory.

Electrophysiology acquisition

Carandini-Harris laboratory

Electrophysiology data were acquired using SpikeGLX (https://billkarsh.github.io/SpikeGLX/, versions 20190724, 20201012, 20201103, and 2022101). During the experiments, mice were typically head-fixed and exposed to sensory stimuli (e.g., visual stimuli such as natural images) or engaged in a task (Coen et al., 2023). The ground/reference was directly connected to the headplate of the animal.

Churchland laboratory

Electrophysiology data were acquired using SpikeGLX (https://billkarsh.github.io/SpikeGLX/, version 20201103). During the experiments, mice were head-fixed while performing the IBL task (International Brain Laboratory et al., 2021). A bone screw implanted over the cerebellum was used for ground/reference.

Kullman/Lignani laboratories

The animal was briefly anaesthetised (4% isoflurane) to connect the probe ground and skull screw pins, the probe headstage and ZIF connector, and the recording cable and headstage at the omnetics connector. A small loop (~5 cm) of recording cable was fastened to the side of the implant using parafilm (Figure 4A) to ensure forces exerted on the cable were transmitted to the body of the implant and not the fragile ZIF connector. The entirety of the recording cable was attached to a nylon cable using knots of nylon thread spaced at ~ 30 cm intervals along the recording cable. The cable was slack relative to the nylon thread so that the animal could freely explore and rotate without introducing excessive tension and knotting into the cable (Aery Jones, 2023). Data were acquired using SpikeGLX (https://billkarsh.github.io/SpikeGLX/, version 20190724).

The animal was allowed to recover and freely navigate its home cage which was located inside a small Faraday container. During recording sessions, the experimenter rotated the cable to match the animal's rotational movements, to propagate twists along the full length of the cable and reduce localized tangling and cable stress near the implant.

Data processing

Sessions were automatically spike-sorted using pyKilosort (https://github.com/MouseLand/pykilosort, python port of Kilosort (Pachitariu et al., 2016) version 2.0) and automatically curated using Bombcell (Fabre et al., 2023)).

A variety of parameters were used to select high-quality units, based either on their waveform and their spiking properties.

The template waveform-based criteria were: (1) a maximum of 2 peaks and 1 trough, (2) a spatial decay slope below -3 $\mu V.\mu m^{-1}$, defined as the slope of a linear fit (using the MATLAB *polyfit* function) between the maximum absolute amplitude of the peak channel and nearest 5 channels along the length of the probe (i.e., 75µm away for Neuropixels 2.0), (3) a duration between 0.1ms and 0.8ms, (4) a trough preceding the template peak, to eliminate axonal spikes (Deligkaris et al., 2016), (5) fluctuations during baseline not exceeding 30% of the peak amplitude. The raw waveform based criteria, computed using at least 1000 randomly sampled spikes, were: (1) a minimum mean amplitude of 20 µV, and (2) a minimum mean signal-to-noise ratio of 0.1, defined as the absolute maximum value divided by the baseline variance.

The spiking properties-based criteria were: (1) a minimum of 300 spikes, (2) less than 20% of spikes missing, estimated by fitting a Gaussian to the spike amplitude distribution with an additional cut-off parameter below which no spikes are present, (3) a maximum of 10% refractory period violations, using a previously published approach (Hill et al., 2011), defining the censored period as 0.1ms and estimating the refractory period using a window between 0.5 and 10ms, and (4) a minimum presence ratio of 0.2, defined as the fraction of 1-min bins with at least one spike.

Data analysis

Raw traces (Figure 2C,D, Figure 4C) were obtained by bandpass filtering each channel from spikeGLX between 400 and 9000 Hz (using the MATLAB *bandpass* function) and subtracting the median across channels.

To obtain the total number of spikes per second at each depth along the probe (Figure 2E,F), we summed spikes across all units present within each 20 µm depth bin.

In the case of Neuropixels 2.0 probes, we estimated the number of recorded units for a probe on a given day (Figure 3A,B) by summing units from a complete set of independently recorded banks—a set of channel banks that tiled the entirety of the implanted probe. Because each such set was recorded across at least two days, we used the closest recordings within a window of five days, centered on the day of interest. Days were excluded if it was not possible to form a complete set of banks within a five-day window.

To obtain P the percentage change in unit count N_d across days d (Figure 3C,D), we fit an exponential decay function to the number of units detected on each bank across days and extracted the decay parameter τ:

$$N_d = N_0 10^{\tau d}$$

P was defined as:

$$P = 100 \times \left(\frac{N_{d+1}}{N_d} - 1\right) = 100 \times (10^{\tau} - 1)$$

For Neuropixels 2.0 probes, P was averaged across all longitudinally recorded banks from each implantation to obtain a single value.

To estimate the effect of repeated probe use, U, and antero-posterior and medio-lateral insertion coordinates (Y and X) on the percentage change in unit count across days, we used a linear mixed effects model (using the MATLAB *fitlme* function):

$$P \sim 1 + Y + X + U + (1|\mathrm{probeID}) + (U - 1|\mathrm{probeID})$$

Here, P is the response variable, Y, X, and U are fixed effect terms, and $\mathrm{probeID}$ (the probe identity) is the single grouping variable. We then assessed whether Y, X, or U had a significant effect on the response variable.

Code & data availability

The CAD files for the implant, and detailed instructions for implantation and construction are available at https://github.com/Coen-Lab/chronic-neuropixels.

All code and data will be available upon peer-reviewed publication.

References

Aery Jones, E.A. (2023). Freely moving recording: Chronic recoverable Neuropixels in mice. Protocols.Io.

Allen, W.E., Chen, M.Z., Pichamoorthy, N., Tien, R.H., Pachitariu, M., Luo, L., and Deisseroth, K. (2019). Thirst regulates motivated behavior through modulation of brainwide neural population dynamics. Science *364*, 253.

Berényi, A., Somogyvári, Z., Nagy, A.J., Roux, L., Long, J.D., Fujisawa, S., Stark, E., Leonardo, A., Harris, T.D., and Buzsáki, G. (2014). Large-scale, high-density (up to 512 channels) recording of local circuits in behaving animals. J Neurophysiol *111*, 1132–1149.

Claudi, F., Petrucco, L., Tyson, A., Branco, T., Margrie, T., and Portugues, R. (2020). BrainGlobe Atlas API: a common interface for neuroanatomical atlases. J. Open Source Softw. *5*, 2668.

Coen, P., Sit, T.P.H., Wells, M.J., Carandini, M., and Harris, K.D. (2023). Mouse frontal cortex mediates additive multisensory decisions. Neuron.

Deligkaris, K., Bullmann, T., and Frey, U. (2016). Extracellularly Recorded Somatic and Neuritic Signal Shapes and Classification Algorithms for High-Density Microelectrode Array Electrophysiology. Front. Neurosci. *10*, 421.

Denk, W., Strickler, J.H., and Webb, W.W. (1990). Two-Photon Laser Scanning Fluorescence Microscopy. Science *248*, 73–76.

Dombeck, D.A., Harvey, C.D., Tian, L., Looger, L.L., and Tank, D.W. (2010). Functional imaging of hippocampal place cells at cellular resolution during virtual navigation. Nat. Neurosci. *13*, 1433–1440.

Driscoll, L.N., Pettit, N.L., Minderer, M., Chettih, S.N., and Harvey, C.D. (2017). Dynamic Reorganization of Neuronal Activity Patterns in Parietal Cortex. Cell *170*, 986-999.e16.

Fabre, J.M.J., Beest, E.H. van, Peters, A.J., Carandini, M., and Harris, K.D. (2023). Bombcell: automated curation and cell classification of spike-sorted electrophysiology data. Zenodo.

Ferguson, J.E., Boldt, C., and Redish, A.D. (2009). Creating low-impedance tetrodes by electroplating with additives. Sens. Actuators A: Phys. *156*, 388–393.

Helmchen, F., and Denk, W. (2005). Deep tissue two-photon microscopy. Nat. Methods *2*, 932–940.

Hill, D.N., Mehta, S.B., and Kleinfeld, D. (2011). Quality Metrics to Accompany Spike Sorting of Extracellular Signals. J. Neurosci. *31*, 8699–8705.

International Brain Laboratory, Aguillon-Rodriguez, V., Angelaki, D., Bayer, H., Bonacchi, N., Carandini, M., Cazettes, F., Chapuis, G., Churchland, A.K., Dan, Y., et al. (2021). Standardized and reproducible measurement of decision-making in mice. ELife *10*, e63711.

International Brain Laboratory, Benson, B., Benson, J., Birman, D., Bonacchi, N., Carandini, M., Catarino, J.A., Chapuis, G.A., Churchland, A.K., Dan, Y., et al. (2023). A Brain-Wide Map of Neural Activity during Complex Behaviour.

Juavinett, A.L., Bekheet, G., and Churchland, A.K. (2019). Chronically implanted Neuropixels probes enable high-yield recordings in freely moving mice. Elife *8*, e47188.

Jun, J.J., Steinmetz, N.A., Siegle, J.H., Denman, D.J., Bauza, M., Barbarits, B., Lee, A.K., Anastassiou, C.A., Andrei, A., Aydın, Ç., et al. (2017). Fully integrated silicon probes for high-density recording of neural activity. Nature *551*, 232.

Lee, J.J., Krumin, M., Harris, K.D., and Carandini, M. (2022). Task specificity in mouse parietal cortex. Neuron *110*, 2961-2969.e5.

Luo, T.Z., Bondy, A.G., Gupta, D., Elliott, V.A., Kopec, C.D., and Brody, C.D. (2020). An approach for long-term, multi-probe Neuropixels recordings in unrestrained rats. ELife *9*, e59716.

Mayerich, D., Abbott, L., and McCormick, B. (2008). Knife-edge scanning microscopy for imaging and reconstruction of three-dimensional anatomical structures of the mouse brain. J. Microsc. *231*, 134–143.

Mizrahi, A., Crowley, J.C., Shtoyerman, E., and Katz, L.C. (2004). High-Resolution In Vivo Imaging of Hippocampal Dendrites and Spines. J. Neurosci. *24*, 3147–3151.

Niedworok, C.J., Brown, A.P.Y., Cardoso, M.J., Osten, P., Ourselin, S., Modat, M., and Margrie, T.W. (2016). aMAP is a validated pipeline for registration and segmentation of high-resolution mouse brain data. Nat. Commun. *7*, 11879.

Pachitariu, M., Steinmetz, N., Kadir, S., Carandini, M., and D., H.K. (2016). Kilosort: realtime spike-sorting for extracellular electrophysiology with hundreds of channels. Biorxiv 061481.

Pinto, L., Rajan, K., DePasquale, B., Thiberge, S.Y., Tank, D.W., and Brody, C.D. (2019). Task-Dependent Changes in the Large-Scale Dynamics and Necessity of Cortical Regions. Neuron *104*, 810-824.e9.

Ragan, T., Kadiri, L.R., Venkataraju, K.U., Bahlmann, K., Sutin, J., Taranda, J., Arganda-Carreras, I., Kim, Y., Seung, H.S., and Osten, P. (2012). Serial two-photon tomography for automated ex vivo mouse brain imaging. Nat. Methods *9*, 255–258.

Shobe, J.L., Claar, L.D., Parhami, S., Bakhurin, K.I., and Masmanidis, S.C. (2015). Brain activity mapping at multiple scales with silicon microprobes containing 1,024 electrodes. J. Neurophysiol. *114*, 2043–2052.

Steinmetz, N.A., Zatka-Haas, P., Carandini, M., and Harris, K.D. (2019). Distributed coding of choice, action and engagement across the mouse brain. Nature *576*, 266–273.

Steinmetz, N.A., Aydin, C., Lebedeva, A., Okun, M., Pachitariu, M., Bauza, M., Beau, M., Bhagat, J., Böhm, C., Broux, M., et al. (2021). Neuropixels 2.0: A miniaturized high-density probe for stable, long-term brain recordings. Science *372*, eabf4588.

Stringer, C., Pachitariu, M., Steinmetz, N., Reddy, C., Carandini, M., and Harris, K.D. (2019). Spontaneous behaviors drive multidimensional, brainwide activity. Science *364*, eaav7893.

Tseng, S.-Y., Chettih, S.N., Arlt, C., Barroso-Luque, R., and Harvey, C.D. (2022). Shared and specialized coding across posterior cortical areas for dynamic navigation decisions. Neuron *110*, 2484-2502.e16.

Tyson, A.L., Vélez-Fort, M., Rousseau, C.V., Cossell, L., Tsitoura, C., Lenzi, S.C., Obenhaus, H.A., Claudi, F., Branco, T., and Margrie, T.W. (2022). Accurate determination of marker location within whole-brain microscopy images. Sci. Rep. *12*, 867.

Urai, A.E., Doiron, B., Leifer, A.M., and Churchland, A.K. (2022). Large-scale neural recordings call for new insights to link brain and behavior. Nat. Neurosci. *25*, 11–19.

van Daal, R.J.J., Aydin, Ç., Michon, F., Aarts, A.A.A., Kraft, M., Kloosterman, F., and Haesler, S. (2021). Implantation of Neuropixels probes for chronic recording of neuronal activity in freely behaving mice and rats. Nat Protoc *16*, 3322–3347.

Wang, Q., Ding, S.-L., Li, Y., Royall, J., Feng, D., Lesnar, P., Graddis, N., Naeemi, M., Facer, B., Ho, A., et al. (2020). The Allen Mouse Brain Common Coordinate Framework: A 3D Reference Atlas. Cell *181*, 936-953.e20.